Summary of Work
PL 2551, Co. Wexford
Gold Fertility Analysis – Boley Prospect
IMC Exploration Group PLC

Dr. Seán H. McClenaghan
B.Sc., M.Sc., M.A., Ph.D., FSEG
Assistant Professor Economic Geology
Director Geoscience Programme
Manager Raw Materials Laser Ablation ICP-MS Laboratory

e-mail: mcclens@tcd.ie | Tel: +353 1 896 1585 | Mobile: +083 854 9810
Trinity College Dublin, School of Natural Sciences, Department of Geology
College Green, Dublin 2, Ireland

Executive Summary

- Lithological reassessment of intervals from DDH 24-2551-01 identified several sulphide bearing quartz veins with potential for the detection of trace hydrothermal signatures for potential Au fertility and vectoring assessment.

- Petrographic examination of polished sections reveal a broad mineralogical association of Chalcopyrite-Galena-Pyrite-Arsenopyrite prospective for Au mineralization.

- Microscopic confirmation of quartz-vein hosted lode gold in bedrock intersected by IMC Exploration drillhole 24-2551-01 at a depth of 90.5m.

- Microscopic examination of Boley sections reveals a high abundance of Bismuth-Tellurides and Tetrahedrite associated with Chalcopyrite and Au grains.

- Electron Dispersive X-ray analyses reveal an Au-rich Electrum ($Au_{91}Ag_{09}$) composition for the Au grains identified in polished Boley Sections from veins at 90.5m.

- Mineralogical signature is indicative of an Orogenic Au signature consistent with regional occurrence of visible Au grains in quartz veins across PL2551.

- Laser-Ablation ICP-MS analyses of pyrite reveal significant enrichment of Au up to 248 g/t (8.7 Oz/ton) representing one of the highest recorded Pyrite-Au signatures for Caledonian terranes, with average values of 32.7 g/t Au spanning a broad zone between depths of 88.5 m and 139.7m; signatures are similar to pyrite phases hosting Au at the Curraghinalt deposit, Dalradian Terrane.

- Mineralogical and micro-analytical assessment of the Boley Quartz veins indicate significant Au fertility in the region and the presence of broader orogenic Au mineralization.

- Discrete Au-bearing quartz veins intersected in drillhole 24-2551-01 likely represent the distal extent of a larger orogenic gold trend.

- Abundance of pyrite and chalcopyrite in quartz veins prove to be the most effective vectors for exploration on PL2551.

- Lithogeochemical vectoring should focus on Bi, Te, Cu, As, Sb, Pb, Ag and Au as vectors toward orogenic Au mineralization.

Introduction:
PL 2551 is a Wexford license held by IMC exhibiting excellent potential for Orogenic Au resources along several unresolved trends. PL 1200 Clough-Churchtown traces a Cu-Pb-Zn horizon equivalent to the Avoca Trend. Extensive exploration has been carried out by Arkle Resources to the north along a contiguous trend that may extend to the Boley Occurrence on PL 2551. Three key occurrences have been targeted in the past, these are:

- Kilmichael/Ballyowen/Ballygarrett prospects
- Knockbrandon
- Boley

Mineralization potential lies in tectonically emplaced quartz veins containing sulphides and associated gold including multiple historical samples of coarse visible Au in quartz float. Regional geology is dominated by sedimentary rocks of the Cambro-Ordovician Ribband Group and overlying volcanics of the Ordovician Duncannon Group. Rocks along the Caledonian trend have been tectonically imbricated by the Acadian Orogeny which imparts a strong penetrative S0/S1 fabric generally orientated NE-SW along the prominent trend. Sections of the Duncannon Volcanic Suite can be prospective for base-metal mineralization, but much of the mineralization potential on PL2551 relates to epithermal-orogenic Au occurrences. Mineralization can be found principally in tectonically emplaced quartz veins along the Duncannon Group at various orientations to penetrative fabrics, most notably Late retrograde D-veins transecting S_0/S_1 similar to auriferous veins targeted at the Curraghinalt Au deposit.

Multiple holes drilled by IMC Exploration PLC Limited have targeted historical Au occurrences on PL2551. In 2016, drilling proceeded on the Boley occurrence (DDH IMC-2551-04) following up on coincident high-grade float and stream sediment anomalies. The drill hole intersected a significant mineralized zone with bonanza grade Au at 354 g/t between 11.5 to 13.0m within grey-green chloritic siltstone with pyrite; grades of 6.2 ppm were intersected between 18.5 and 23.5m. The Bonanza grade sample was subsequently interpreted as buried mineralized float intersected during drilling of overburden. Given the unresolved nature of this mineralization, IMC Exploration embarked on a follow up drilling campaign to test Interpreted Targets at 65m downhole and 150m downhole with consideration given to deepening the hole to test for an interpreted structure around 250m.

Current Work:
Results submitted in the current report of work on PL2551 focus on an assessment of the Boley Au prospect based on the 2024 drilling campaign and drill hole 24-2551-01. Despite low Au assay results (ALS-Lochrea) from quartz vein sections, the presence of disseminated and vein sulphides in several sections did offer positive indicators. The work contained herein represents a gold fertility study of the area targeted by the two IMC drill holes to assess its prospectivity for Au. Mineralogical characterization and micro-analysis can provide an assessment of both sub-microscopic refractory Au and presence of fine-grained Au grains not visible by conventional methods. Furthermore, characterization of mineralogical assemblages can allow for modelling of the style of Au mineralization (Intrusion-Related versus Orogenic Au types). A wide range of methods were employed to carry out the assessment at the Trinity

College Raw Materials Characterization Laboratory and iCRAG Labs @ TCD; analytical methods included:

- Conventional Reflected Light Microscopy
- Scanning Electron Microscopy (SEM)
- SEM – Feature Analysis
- Electron-Dispersive X-Ray (EDX) Analysis
- Laser Ablation Inductively Coupled Plasma - Mass Spectrometry (ICP-MS)
    - Spot analyses
    - Mapping Analyses

Use of microscopic and microanalytical techniques required careful preparation of oriented materials to enable examination of prospective quartz veins; preparation methods included:

- Rock Saw Cutting of drill core
- Surface Grinding
- Epoxy Resin Mounting
- Mount Polishing
- Carbon Coating (SEM preparation)

All sample preparation and micro-analyses were carried out by Dr. Sean McClenaghan, Assistant Professor Trintiy College Dublin.

Assessment of Boley Mineralisation:
Prior to advanced micro-analysis, a lithological re-examination was carried out on drill core from DDH 24-2551-01 (collared on the Boley Prospect) to correlate drill hole assays (ALS Lochrea) with any sulphide anomalous quartz vein intersections. Quartz vein intersections in 24-2551-01 were closely examined with a hand lens under natural light at the IMC Exploration office in Ballybough, Dublin. Drill core required a thorough washing to remove excess mud present on the core; this may have inhibited recognition of some sulphide sections during initial logging.

Drill hole 24-2551-01 intersected an overturned sequence of ribband Group sedimentary rocks structurally overlying volcaniclastic sedimentary units of the Duncannon Group. This represents an overall stratigraphic succession, but the level of deformation observed in drill core indicates significant tectonic modification, with faulting obscuring contact relationships.

Drill hole 24-2551-01 is collared in Ribband Group Sediments comprising pale green, grey to pale maroon fine-grained laminated siltstones becoming maroon dominated at depth; this intersection extends to a depth of 87.5m. Volcaniclastic rocks of the Duncannon Group are intersected from 87.5 to a depth of 172.5m (EOH) and consist of grey-green fine-grained laminated tuffs and shale.

Both the Ribband and Duncannon Group sections exhibit varying degrees of quartz veining (Table 1) at varying angles to the dominant penetrative S_0/S_1 fabric (~45° / core axis). Hydrothermal alteration was not prevalent in the section aside from Chlorite observed in the selvages of quartz veins; the Duncannon Group volcanic rocks exhibit only low to moderate

greenschist facies metamorphism consistent with the overall Caledonian trend (Acadian Orogeny).

Veins in the Ribband Group sedimentary sequence are quartz dominant but accompanied by some minor calcite in upper intersections. No sulfides or gold grains were identified in any of the quartz-dominant veins.

Veins in the structurally lower Duncannon section are Quartz dominant and comprise multiple cross-cutting generations. Selvages around quartz veins and epidote-chlorite selvages were closely examined for mineralization. Veins were for the most part barren with no indications of mineralization, but several narrow zones exhibit pyrite as disseminations and boudinaged veinlets. Sections are accompanied by chalcopyrite and a possible glint of visible gold (<0.1 mm) in a quartz vein breccia (split-section submitted for bulk assay). Pyrite is also found on the cleavage surfaces bounding high angle late transecting D-veins.

Table 1: Summary of prospective Quartz Vein Intervals Examined, DDH 24-2551-01

From (m)	To (m)	Interval (m)	Lithology
24.4	24.62	0.22	Quartz Vein; Barren
43	44	1	High Angle Shear Zone - Quartz Vein: Barren
54.4	55	0.6	Quartz Vein Breccia; Barren
87.5	88.5	1	trace sulphide in sediment; pyrite
88.5	89.5	1	minor sulphide in sediment; pyrite veinlets
89.5	90.5	1	minor sulphide in sediment; pyrite in late vein
90.5	91.5	1	minor sulphide in sediment; pyrite, chalcopyrite
91.5	92.5	1	minor sulphide in sediment
92.5	93.5	1	minor sulphide in sediment
102.7	103	0.3	Quartz Veins > 50% veining; Barren
139.5	140.5	1	Quartz Veins > 50% veining; Pyrite
140.5	142.5	2	Quartz Veins > 50% veining; Barren
142.5	144.5	2	Quartz Veins > 50% veining; Barren
144.5	146.5	2	Quartz Veins > 50% veining; Barren
146.5	148.5	2	Quartz Veins > 50% veining; Barren
148.5	149.5	1	Quartz Veins > 50% veining; Barren
149.5	150.5	1	Quartz Veins > 50% veining; Barren
150.5	151.5	1	Quartz Veins > 50% veining; Barren
151.5	152.5	1	Quartz Veins > 50% veining; Barren
152.5	153.5	1	Quartz Veins > 50% veining; Barren
153.5	155.5	2	Quartz Veins > 50% veining; Barren
155.5	157.5	2	Quartz Veins > 50% veining; Barren
157.5	159.5	2	Quartz Veins > 50% veining; Barren

Note: Highlighted sections were the focus of microanalysis given sufficient sulphide material for characterisation and assessment.

Methodology:

Polished sections were petrographically examined and characterised under reflected light using a NIKON Eclipse LV100ND Light Microscope. Sulphide mineralogy as well as a thorough examination for discrete Au phases was carried out on eight polished mounts representative of quartz-sulphide veins collected from DDH 24-2551-01 at depths of 88.5m, 88.6m, 88.7m, 90.5 m and 139.7m. Additional samples from adjacent intervals were not investigated further, when upon cutting, material was deemed unsuitable for resin mounting. Polished resin mounted samples preclude any transmitted light microscopy, hence characterization of host phases was limited to X-Ray identification during Backscatter Electron Imaging (BSE) of samples.

Polished mounts were carbon-coated and examined using scanning electron microscopy (SEM) at the iCRAG Labs @TCD using Tescan S8000 MIRA4 FEG-SEM with motorised backscatter electron (BSE) and four Oxford Instruments X-Max 170 mm^2 detectors. The operating conditions were 20 kV accelerating voltage, 10 nA beam current and a working distance of 15 mm. Feature Analysis (BSE) Scans were carried out on samples to highlight specific phases as a target for Au, these included Bismuth-Tellurides, Electrum/Gold, Tetrahedrite, Chalcopyrite, and Galena. Feature analysis provided an efficient *first pass* scan of the samples to prioritize areas for BSE imaging.

The aforementioned microscopic examination instructed the selection of targets for Laser Ablation ICP-MS analysis. Laser Ablation ICP-MS was used as a means to assess the fertility of Boley veins through the geochemistry of pyrite.

Contents of ^{34}S, ^{55}Mn, ^{59}Co, ^{60}Ni, ^{63}Cu, ^{66}Zn, ^{69}Ga, ^{71}Ga, ^{73}Ge, ^{74}Ge, ^{75}As, ^{77}Se, ^{82}Se, ^{95}Mo, ^{107}Ag, ^{111}Cd, ^{112}Cd,^{113} In, ^{115}In, ^{118}Sn, ^{121}Sb, ^{124}Sn, ^{125}Te, ^{182}W, ^{197}Au, ^{202}Hg, ^{205}Tl, ^{208}Pb, ^{209}Bi in pyrite were determined. Analyses were performed on a Thermo iCAPQ ICP-MS coupled to a photon machines G2 193nm UV laser with a Helex two-volume cell. The laser ablation system was managed using Chromium-2 software and raw element counts collected through Qtegra. Spots consisted of 35 µm square ablation areas with a fluence of 1.0 J/cm², shot count of 240 and a repetition rate of 8 Hz providing an ablation of 30 seconds for each spot analysis. To ensure sufficient cell washout between ablations, a pause of 30 seconds was used. Dwell times were determined according to anticipated relative elemental abundance, guided by earlier spot tests on both samples and standard reference materials. Multiple analyses of UQAC and MASS-1 sulphide standards were carried out for every 20 sample ablation spots, enabling compensation for instrumental drift throughout the experiment. Raw count data was reduced using Iolite v.4.10.4 software with an Fe internal standard for pyrite. Internal correction factors were applied in Qtegra to account for mass interferences from ^{118}Sn on ^{115}In. Estimates of precision and accuracy using secondary standard UQAC show results to be within 2σ for trace-element results.

Trace element LA-ICP-MS maps of specific pyrite grains were generated using a beam size of 8 µm, a laser repetition rate of 26 Hz, a scanning speed of 13 µm/s, and a fluence of 1.0 J/cm². These element maps were produced by ablating sequential parallel lines of equal length with no overlap. The analyzed isotopic distributions included: ^{34}S, ^{59}Co, ^{60}Ni, ^{63}Cu, ^{75}As, ^{77}Se, ^{107}Ag, ^{115}In, ^{118}Sn, ^{121}Sb, ^{125}Te, ^{197}Au, ^{208}Pb, ^{209}Bi. Individual dwell times for each analyte were

assigned based on their relative abundances, which were determined by performing test line scans on both the samples and standard reference materials. Each trace-element map was bracketed by four MASS-1 and UQAC line scans, conducted using identical laser parameters to those applied during mapping. Data reduction followed a similar protocol as used for spot analyses (internal Fe standard), and trace element distribution maps were generated using the "ColdWarm" colour scheme, with concentration limits adjusted to emphasize internal heterogeneities.

Micro-Analysis:

Samples examined through SEM-BSE imaging identified key phases consistent with Au mineralization spanning several deposit styles (Orogenic-Epithermal, Intrusion, VMS) hosting Au; common phases identified include: Pyrite, Arsenopyrite, Chalcopyrite, Galena, Tetrahedrite, Bismuth-Telluride and Electrum. Identification of phases during BSE imaging sessions were confirmed through X-Ray spectra and Oxford ID software. Due to similar BSE brightness between galena and Bi minerals with that of electrum, identification of gold phases was difficult and tedious. Automated feature (BSE) analysis scans of sections was employed to identify Au signatures, with follow up BSE imaging (Figure 1) of coordinated Au spikes. Electrum grains were typically small (<10 μm) found as free grains in textural association with quartz, chlorite and to a lesser degree with Chalcopyrite and Bismuth-Telluride.

Table 2: SEM-EDX analyses of gold grains DDH 24-2551-01, 90.5 m depth

Label	O (%)	Fe (%)	Ag (%)	Au (%)	Total (%)	Corrected Au (%)	Corrected Ag (%)
6b-2 10841	3.46	5.04	12.21	79.3	100	86.7	13.3
6b-2 12964a	1.64	2.38	6.50	89.5	100	93.2	6.77
6b-2 12964b	1.83	2.23	6.81	89.1	100	92.9	7.10
6b-2 12964c	2.76	2.50	7.56	87.2	100	92.0	7.98
6b-2 12964d	2.15	2.60	8.27	87.0	100	91.3	8.68
6b-2 12964e	1.96	4.05	7.49	86.5	100	92.0	7.97
S-2 4176a	1.53	2.10	6.33	90.0	100	93.4	6.57
S-2 4176b	1.72	2.23	7.00	89.0	100	92.7	7.29
S-2 4176d	1.59	2.00	6.19	90.2	100	93.6	6.42
S-2 4176c	1.64	2.05	6.09	90.2	100	93.7	6.32
S-2 4176e	1.67	2.21	6.16	90.0	100	93.6	6.41
S-2 6205a	1.91	1.70	7.09	89.3	100	92.6	7.36
S-2 6205b	1.78	1.40	6.20	90.6	100	93.6	6.40
S-2 2969	2.26	2.17	19.22	76.4	100	79.9	20.1
S-2 2969b	2.24	2.08	21.34	74.3	100	77.7	22.3
S-1 979	2.01	0.98	7.33	89.7	100	92.4	7.56
S-1 1276	1.90	0.28	7.97	89.9	100	91.9	8.15

Note: Label designated by Oxford Software; Fe contents represent encroaching pyrite phases and filtered in corrected Au and Ag results.

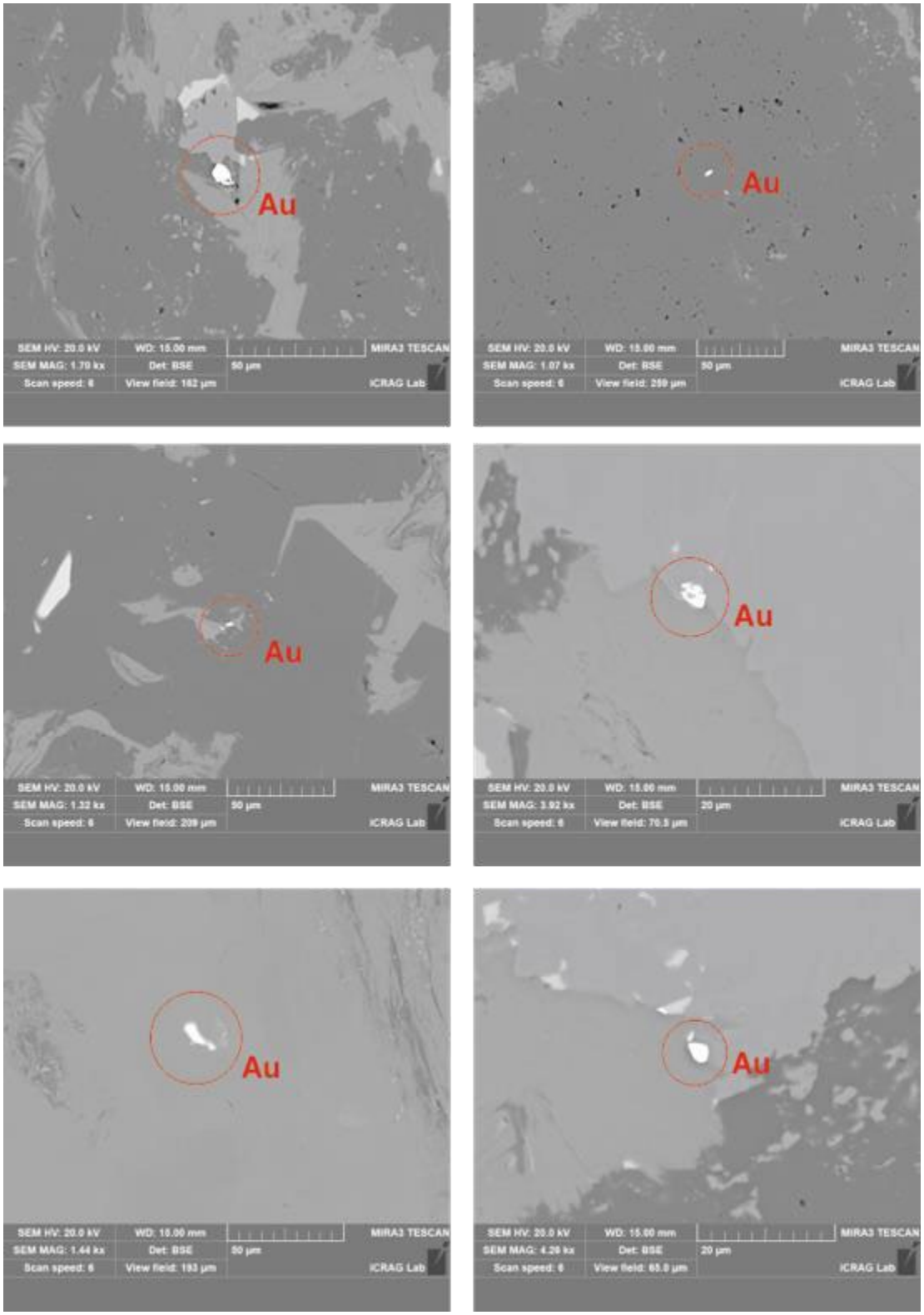

Figure 1: SEM-BSE images of regions containing discrete Au grains hosted predominantly by quartz-chlorite. Phases exhibiting similar brightness (BSE Contrast) consist of Bi-Telluride and galena. EDX analysis of gold grains (Table 2) reveal a gold-rich electrum composition ($Au_{91}Ag_{09}$). All electrum grains shown are found in samples from 90.5m depth.

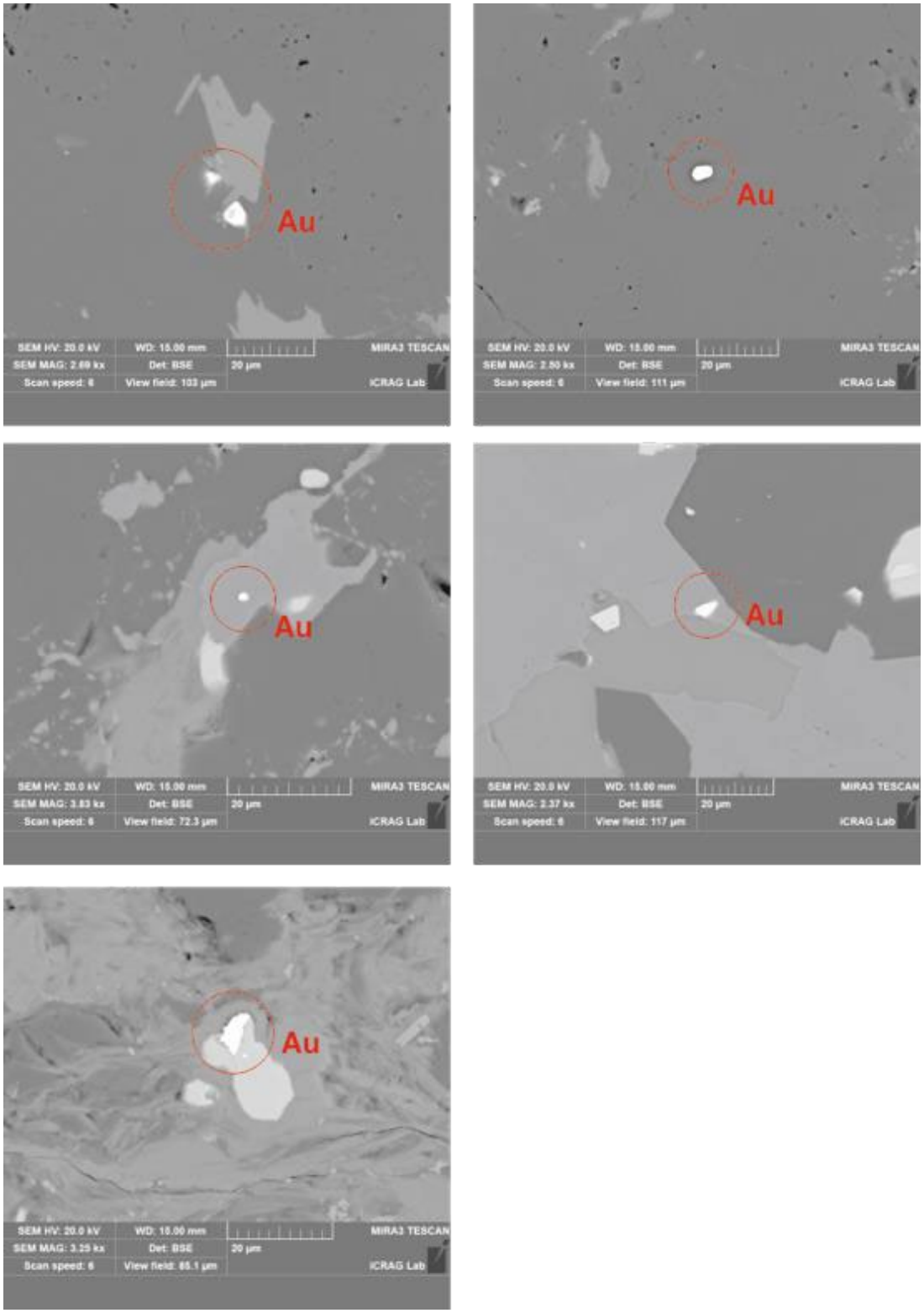

Figure 1: ***Continued***

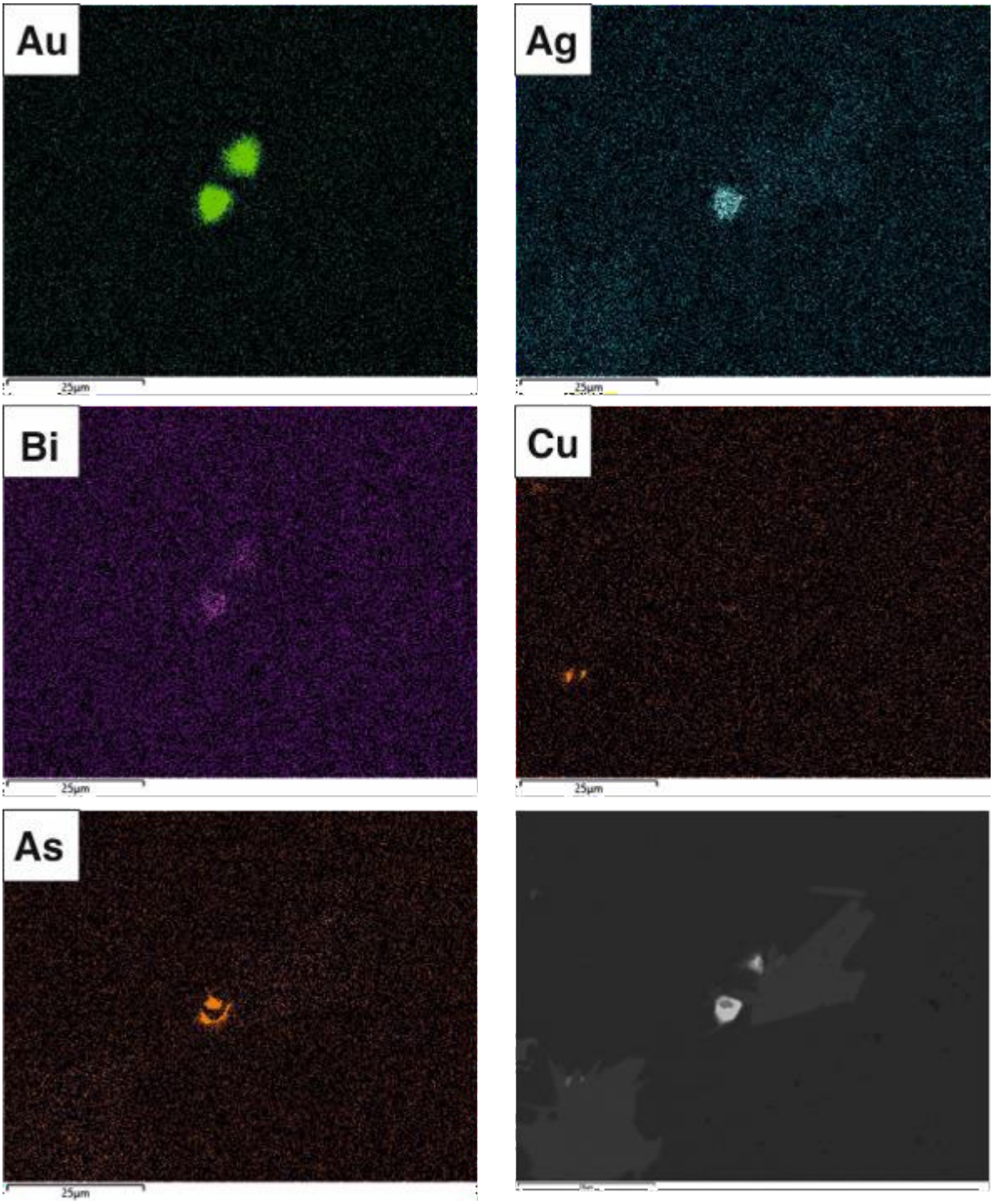

Figure 2: SEM-EDX maps of regions containing discrete Au grains hosted predominantly by quartz-chlorite. Element maps confirm the composition of electrum grains found in samples from 90.5m depth.

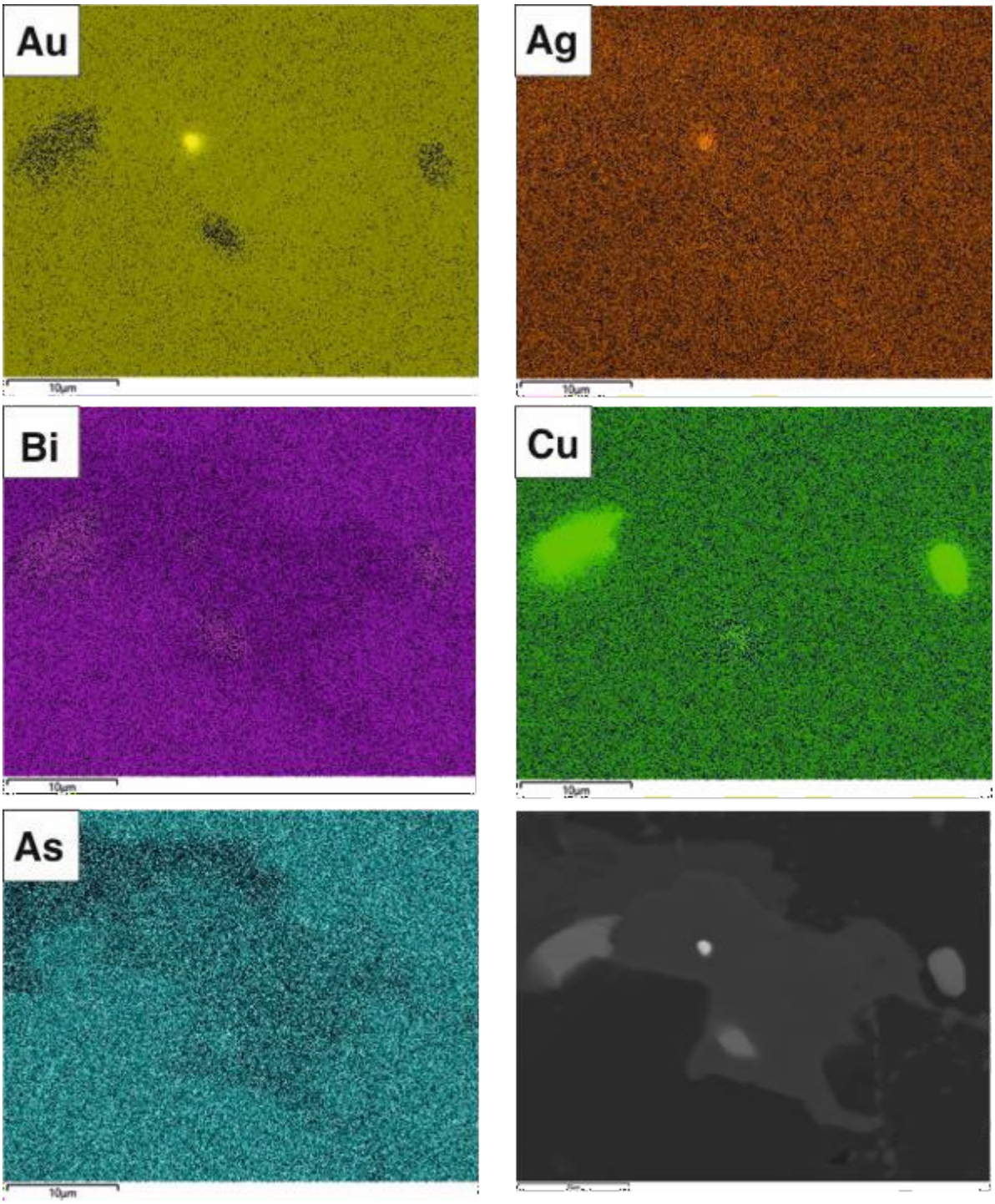

Figure 2: ***Continued***

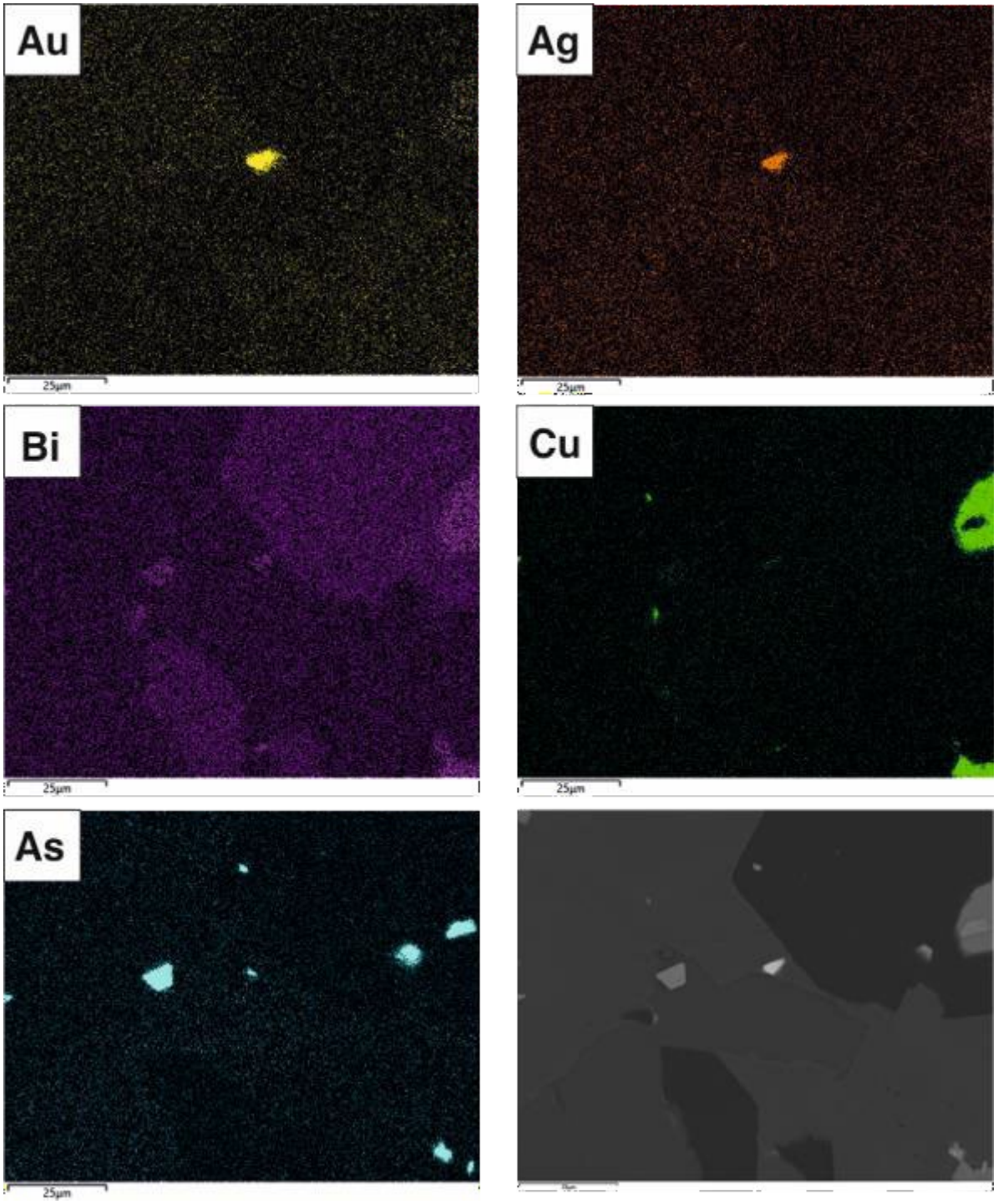

Figure 2: ***Continued***

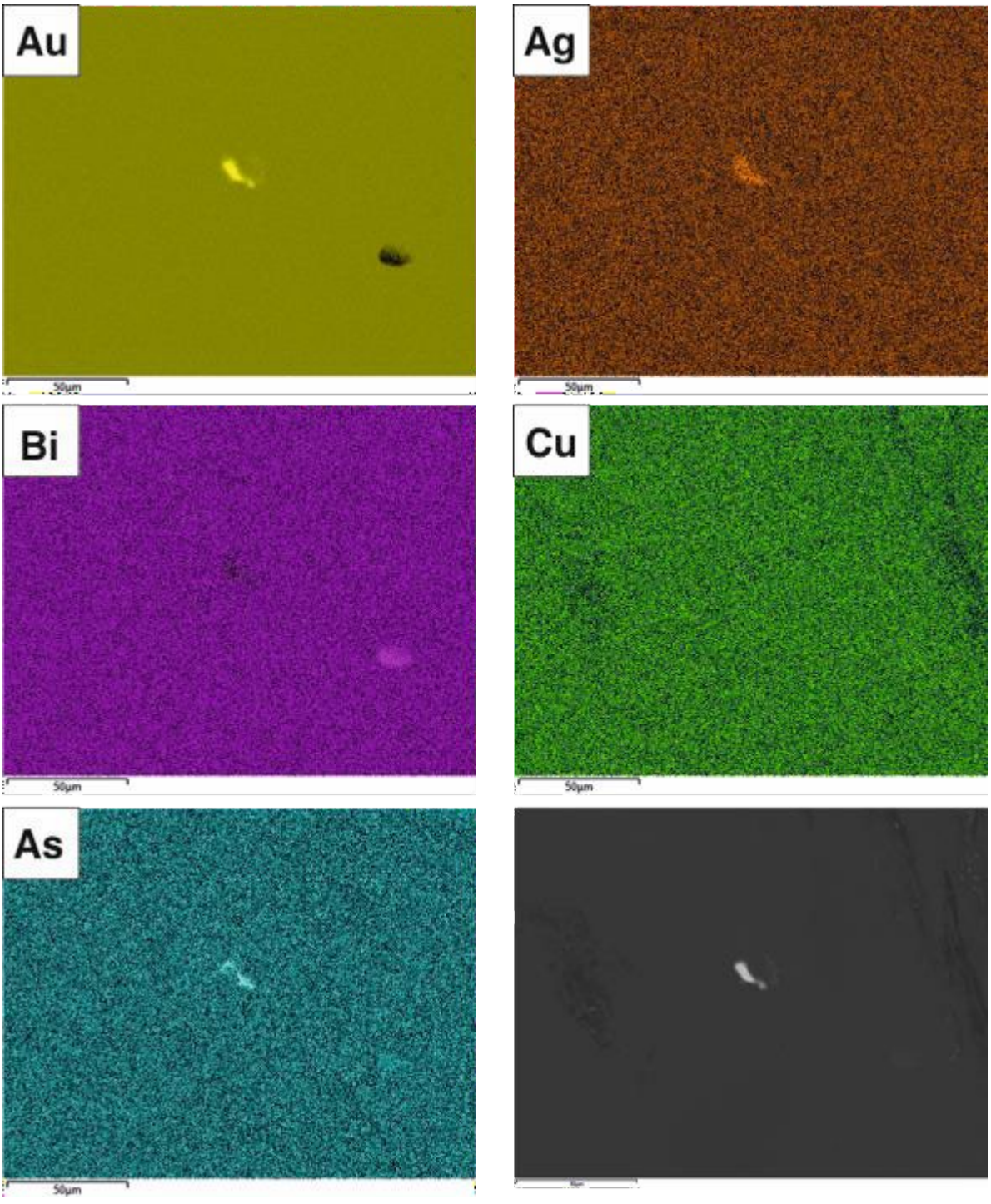

Figure 2: ***Continued***

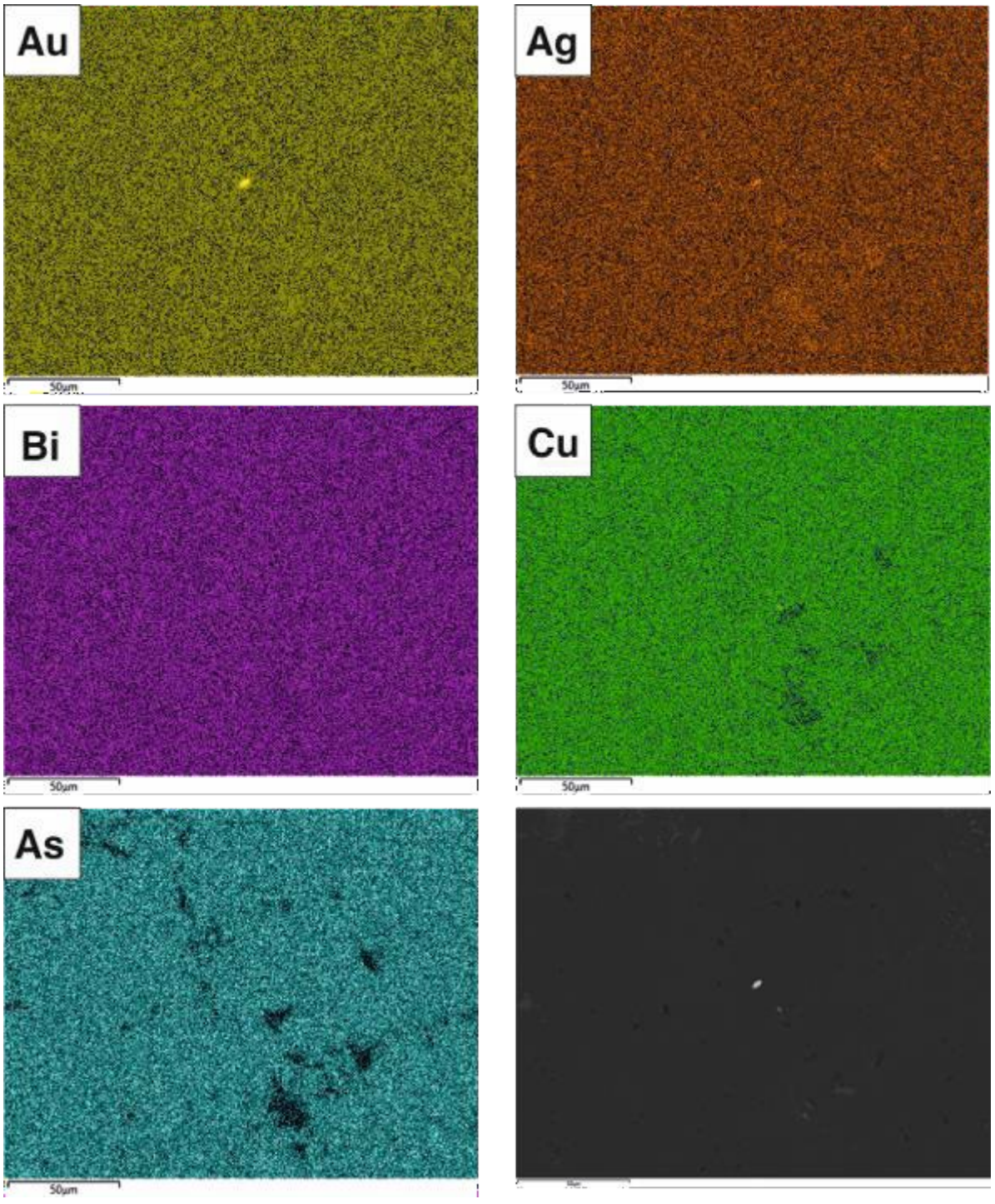

Figure 2: ***Continued***

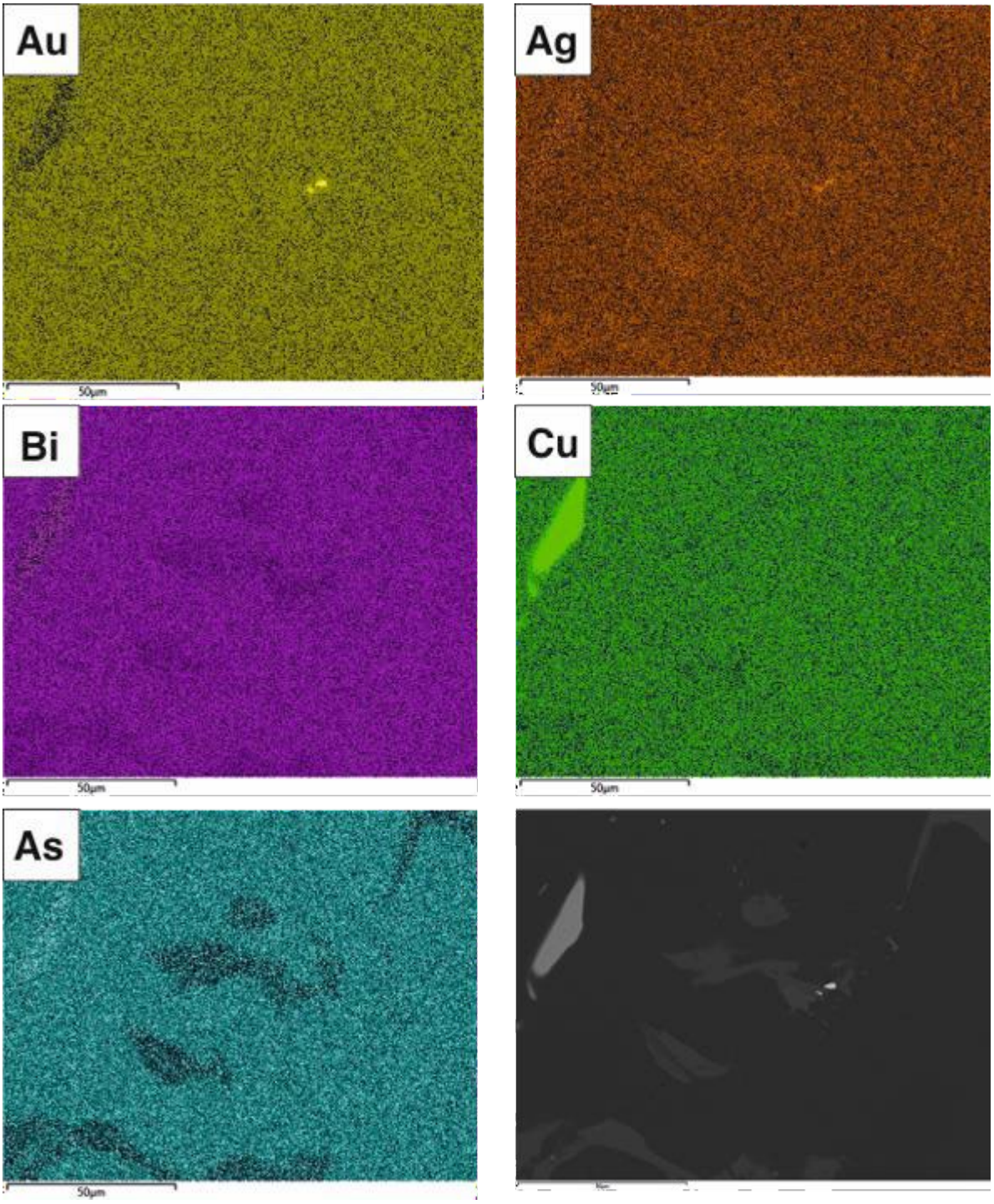

Figure 2: ***Continued***

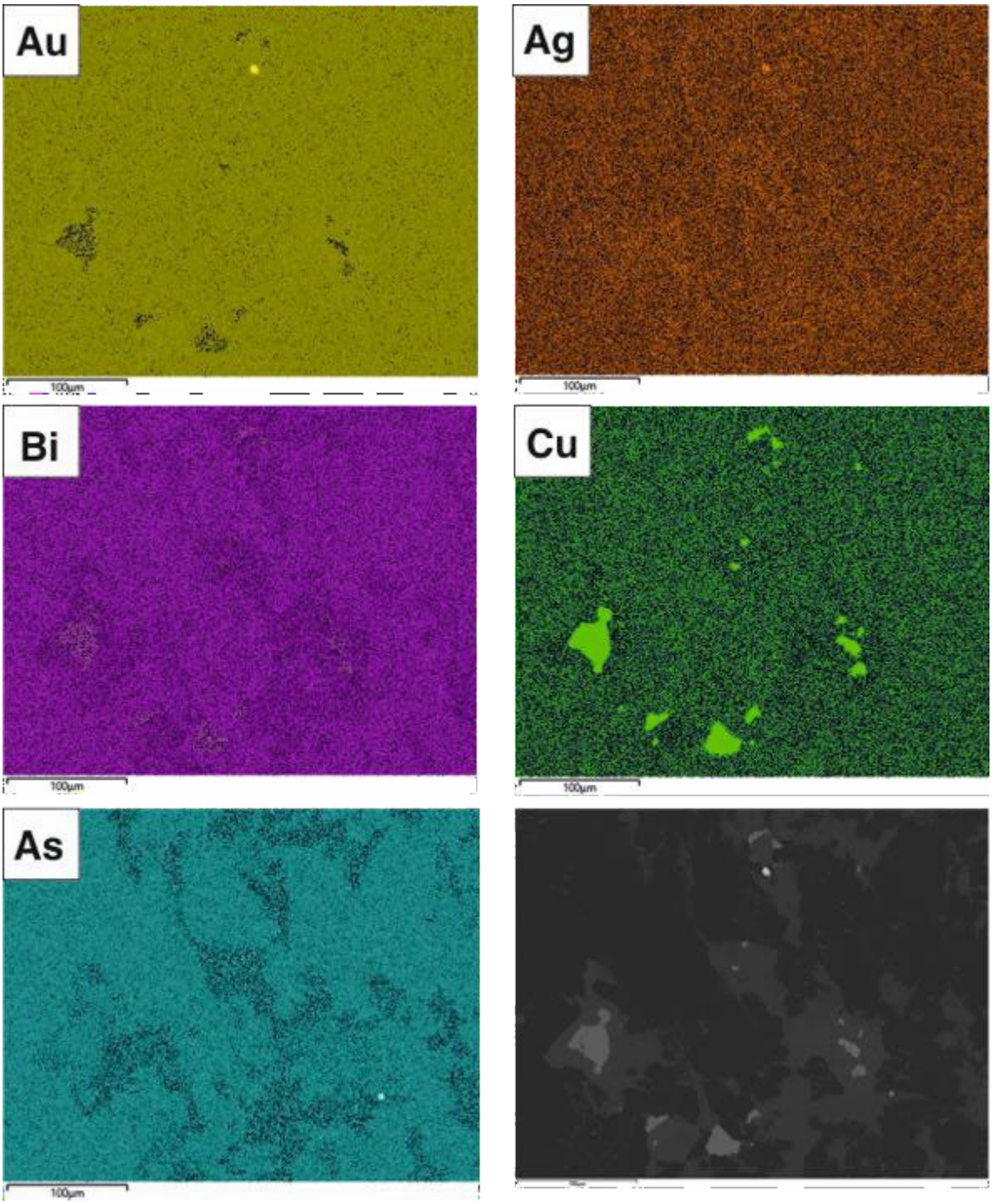

Figure 2: ***Continued***

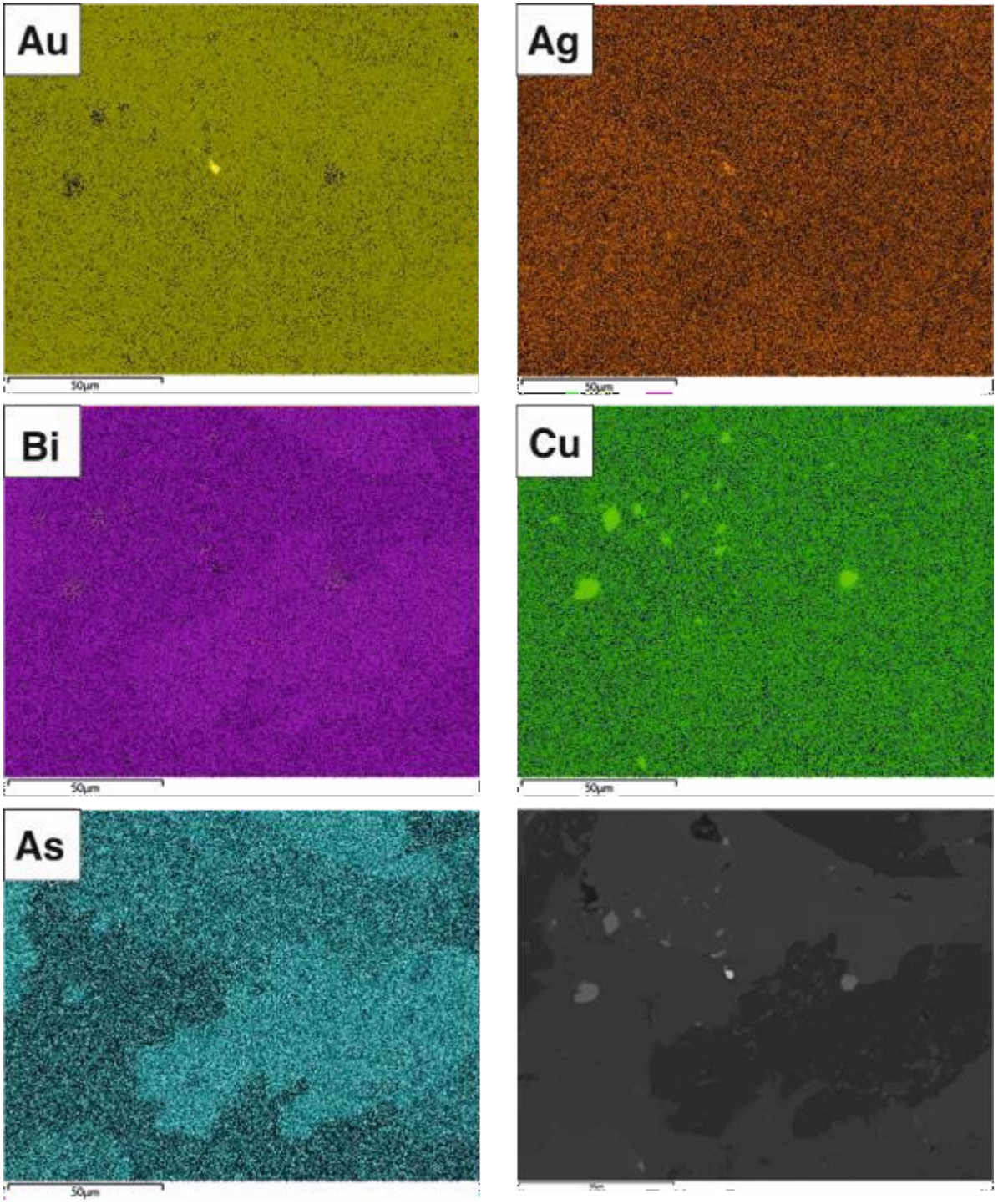

Figure 2: ***Continued***

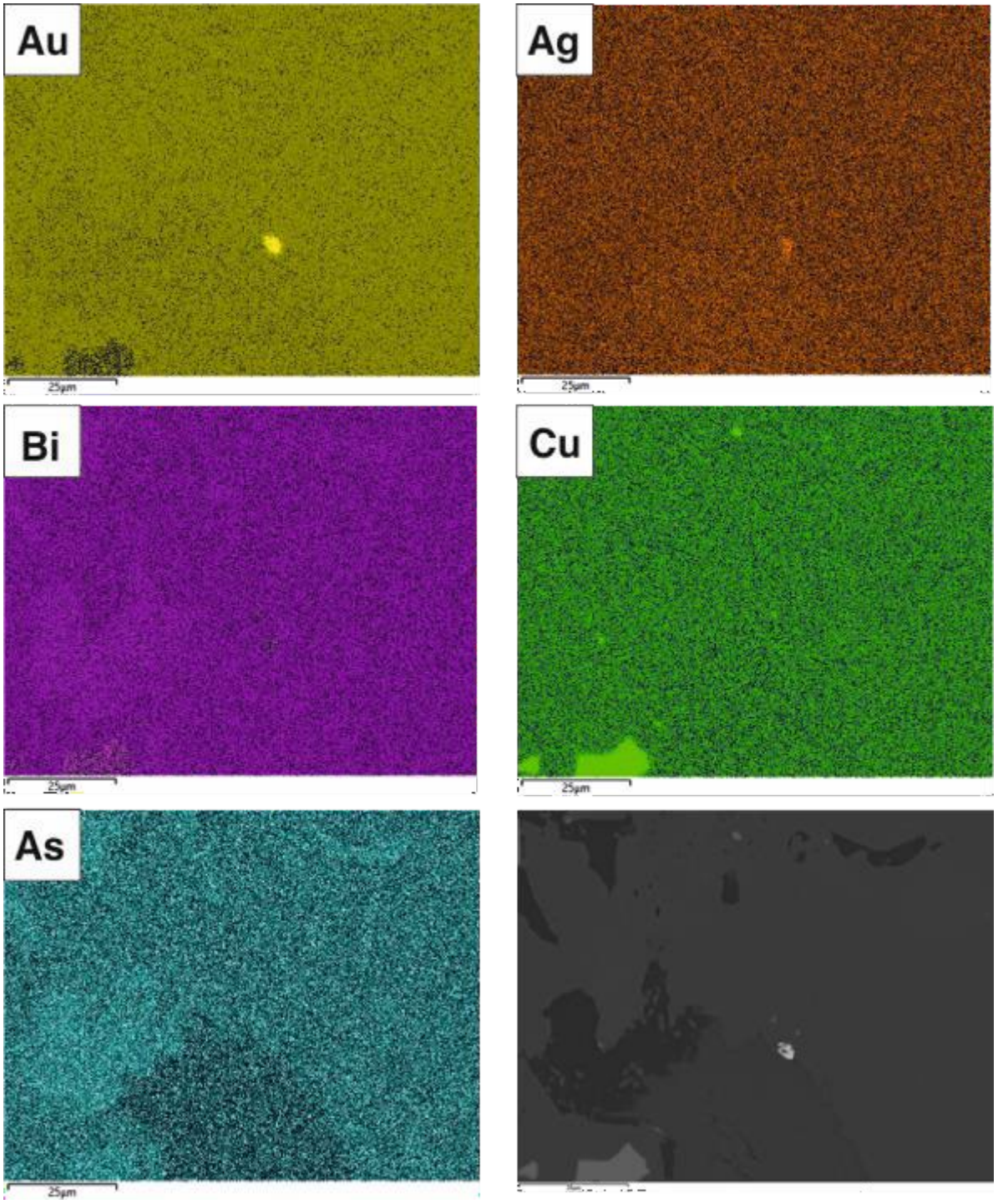

Figure 2: ***Continued***

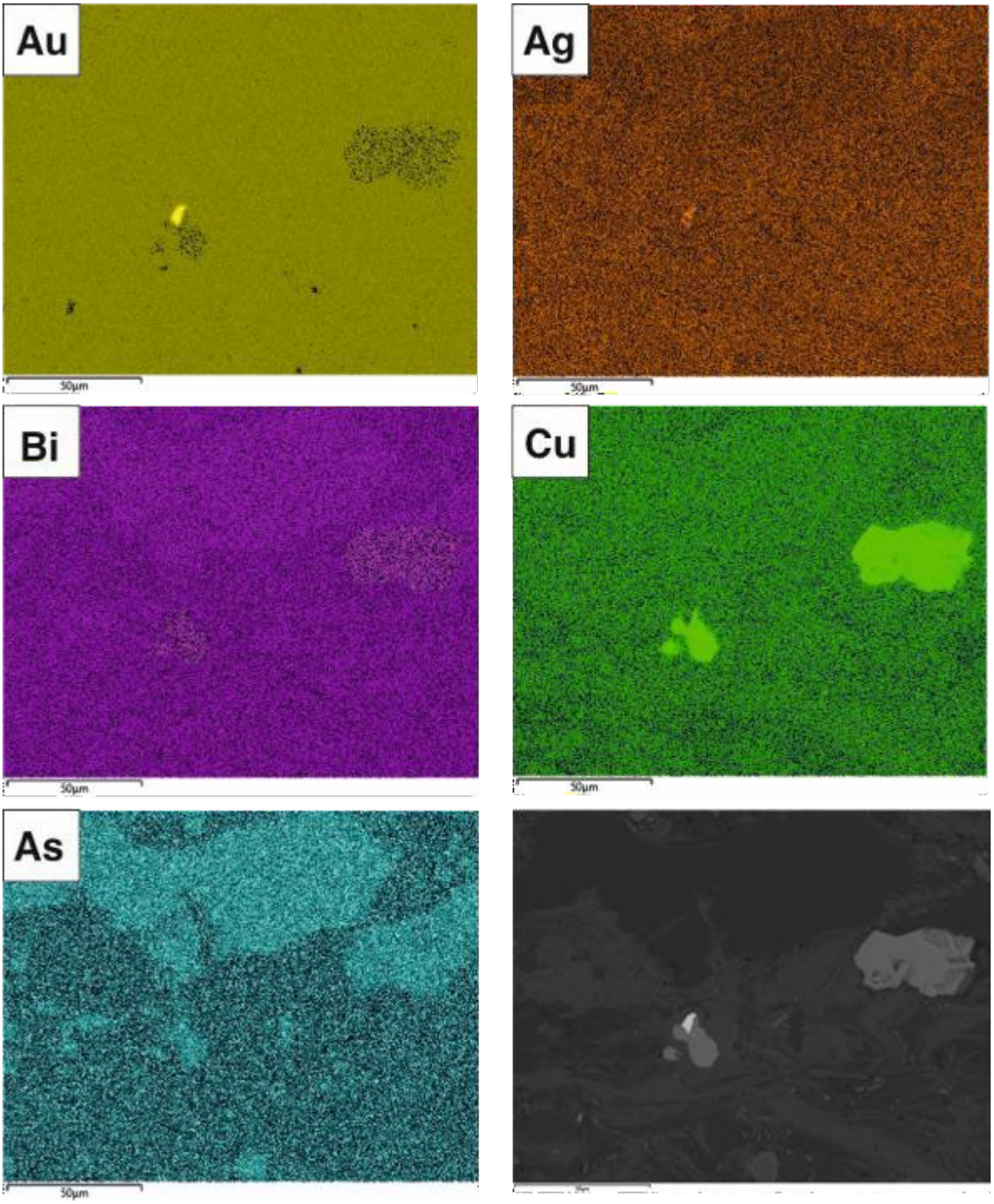

Figure 2: ***Continued***

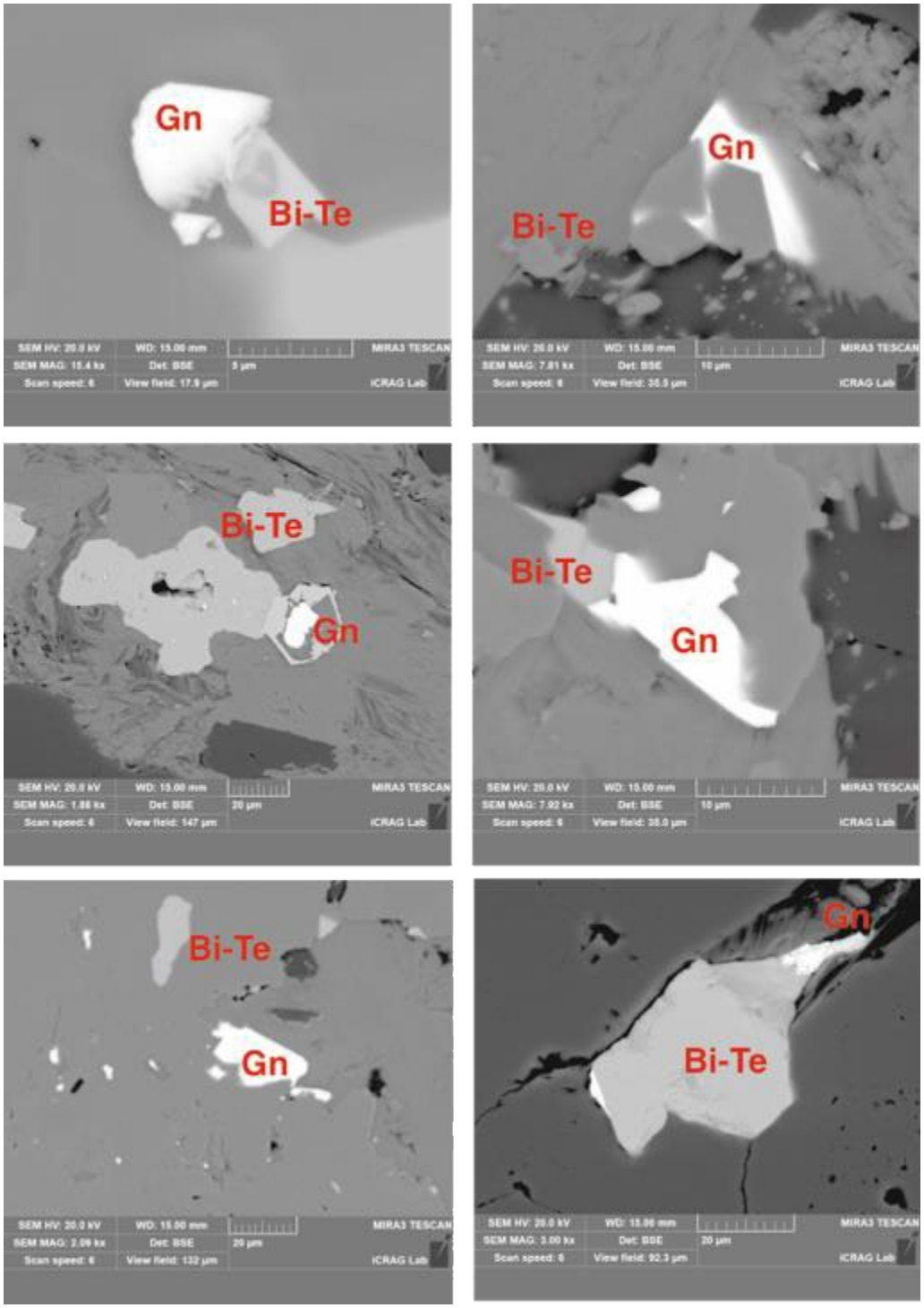

Figure 3: SEM-BSE images of regions displaying the occurrences of Bi-Tellurides and associated galena. All phases shown are found in samples from 90.5m depth.

Electron Dispersive X-ray analyses reveal a consistent Au-rich Electrum ($Au_{91}Ag_{09}$) composition for the Au grains identified in samples from veins at a depth of 90.5m. Although Electrum grains are hosted largely by Chlorite-Quartz, they exhibit a strong spatial association with chalcopyrite, Bi-Telluride and galena in sections, with a notable deficiency in pyrite, relative to other sections. Samples of sulfidic quartz veins from depths of 88.5m, 88.6m, 88.7m and 139.7m were dominated by pyrite-arsenopyrite (Auriferous) with lesser

chalcopyrite and no visible Au phases recognized. These sulphide-rich sections were targeted for trace-element characterisation of pyrite as a means of assessing Au fertility. Pyrite grains in sections were randomly selected across sections to ensure a unbiassed analysis by Laser Ablation ICP-MS; furthermore, both core and rim analyses were included to ensure representative signatures for grains. A total of 260 spot Laser Ablation ICP-MS analyses of pyrite across all sulphide bearing sections (Table 3) reveal significant enrichment of Au up to 248 g/t (8.7 Oz/ton) representing among the highest recorded Pyrite-Au signatures for Caledonian terranes in South-Ireland. Overall, pyrite exhibits median values of 32.7 g/t Au (Figure 4) spanning a broad zone between depths of 88.5 m and 139.7m; these signatures are similar to pyrite signatures hosting Au at the Curraghinalt deposit, Dalradian Terrane. Boley pyrite is Arsenian in nature with median As contents of 2.78% with values as high as 6.08% in quartz veins at depth 139.7m. A positive Spearman Rank correlation between Au and As (r'=0.86) indicates that much of this Au is refractory (Figure 5); a weak negative Au correlation with Ag indicates that electrum exerts minimal influence on the refractory pyrite signatures. Nevertheless, high recorded Au values in a number of analyses exceed the mineral-structural solubility of Au in pyrite and likely represent sub-microscopic inclusions of Au grains. Contents of As in pyrite exhibit a multimodal distribution (Figure 4) with representing several populations of pyrite. These are distributed across all the quartz veins and suggest fluids signatures varied over time. Laser Ablation ICP-MS mapping of pyrite grains (Figure 6) show a strong refractory Au signature despite significant remobilization of Cu, Zn, Sb, Ag and Bi along fracture networks. Near the grain edges and fracture zones, pyrite exhibits depletions, which may indicate some remobilization of Au during stages of tectonism. Tellurium levels in pyrite are relatively low with a median of 0.93 ppm and reaching up to only 9.9 ppm, suggesting a lack of discrete telluride inclusions within grains; a strong positive correlation with Co (r'=0.77) indicates a largely refractory occurrence within pyrite. Tellurium also exhibits a strong positive correlation with Bi (r'=0.84) consistent with the observed association in other sections; concentrations of Bi in pyrite exhibit median contents of 4.70 ppm with levels reaching up to 129 ppm Bi. Laser Ablation ICP-MS mapping of pyrite grains exhibit Bi depletions along rims and zones adjacent fractures, whilst discrete fractures exhibit enrichments in Bi (Figure 6).

Overall, pyrite in quartz veins of the Boley Prospect preserve a strong Au-As-Bi-Te refractory signature, suggesting an Orogenic Au style of mineralization. This is further supported by the occurrence of late tectonic veins bearing auriferous pyrite and veins with free electrum. Although some remobilization within pyrite grains is evident, it may not be acting as the sole source of electrum found in adjacent veins. The pyrite may represent an earlier auriferous sulphide stage that preceded the main emplacement of Au at Boley. Pyrite trace-element signatures may be prove useful in characterizing the potential fertility of quartz vein networks on PL2551. At Boley, auriferous pyrite in vein networks occur proximal to veins containing free electrum. Pyrite trace-element signatures across the 50m Quartz-veined section examined suggest a fertile system for potential Au mineralization. The occurrence of electrum and auriferous pyrite in discrete veins suggest effective Au scavenging and transport during tectonic events recorded in the Duncannon Rocks exposed at Boley. It is the interpretation of this report that Drillhole 24-2551-01 intersects the distal periphery of a more significant Orogenic Au Trend and that IMC Exploration PLC Ltd. may consider deepening this hole or reassess targets along the Boley–Balleygarrett corridor coincident with geophysical anomalies.

Table 3: Summary table of pyrite analyses by Laser Ablation ICP-MS, DDH 24-2551-01

Drill hole	Depth	Statistic	S (ppm)	Co	Ni	Cu	Zn	Ga	Ge	As	Se	Mo	Ag	Cd	In	Sn	Sb	Te	W	Au	Pb	Bi	Ni/Co	Au/Ag	Pb/Zn
24-2551-01	88.5m Vein 1 Pyrite	Min	322012	5.36	26.0	2.97	0.042	0.005	0.110	159	0.280	0.004	0.005	0.010	0.003	0.004	0.061	0.034	0.003	0.296	0.072	0.027	1.09	0.327	0.092
		Median	438680	169	434	53.1	1.45	0.122	0.329	24387	2.05	0.141	0.254	0.317	0.054	0.171	27.0	0.589	1.64	50.9	63.8	3.69	2.96	140	36.7
		Max	583522	1057	4806	1827	301	21.6	7.24	49000	12.2	6.19	7.67	1.61	0.223	1.68	991	4.64	20.3	248	2068	24.0	8.07	2742	6688
		n	50	50	50	50	41	41	50	50	46	31	50	30	45	38	50	48	48	50	50	50	50	50	41
24-2551-01	88.6m Vein 2 Pyrite	Min	261275	12.8	56.5	3.44	0.165	0.003	0.099	46.2	0.560	0.015	0.006	0.049	0.001	0.016	0.304	0.071	0.013	0.051	0.275	0.057	1.02	0.331	0.126
		Median	420738	147	578	29.7	2.45	0.368	0.381	6631	4.19	0.030	0.361	0.262	0.028	0.342	16.7	1.30	2.18	7.03	45.1	5.59	3.04	11.8	19.8
		Max	567904	1388	3722	1262	251	14.7	2.44	47787	10.7	0.683	1.80	1.98	0.109	2.03	57.7	5.35	30.9	134	2157	27.8	18.2	3452	829
		n	60	60	60	60	52	50	60	60	56	25	55	30	53	54	60	60	58	60	60	60	60	55	52
24-2551-01	88.7m Vein 3 Pyrite	Min	316083	66	124	19.6	0.095	0.081	0.196	5221	0.235	0.008	0.053	0.050	0.008	0.004	1.85	0.209	0.021	0.186	12.1	1.04	0.338	0.544	0.152
		Median	438174	1853	2112	102	3.37	0.331	0.558	15468	5.65	0.033	0.54	0.331	0.034	0.774	21.3	2.95	2.43	4.05	65.5	24.5	1.14	9.03	23.0
		Max	537240	11708	7693	602	198	6.86	9.88	40428	10.2	0.342	2.01	1.41	0.089	2.11	55.4	9.9	36.7	22.1	411	129	3.28	96.9	398
		n	50	50	50	50	47	50	50	50	49	20	50	38	50	48	50	50	50	50	50	50	50	50	47
24-2551-01	139.7m Vein 4 Pyrite	Min	296121	0.034	0.129	10.1	0.016	0.004	0.130	15965	0.020	0.005	0.004	0.016	0.018	0.006	0.212	0.003	0.004	11.2	0.116	0.004	0.044	6.92	0.031
		Median	401430	39.8	44.7	51.2	1.75	0.274	0.395	33911	1.77	0.066	0.236	0.184	0.068	0.235	26.7	0.320	2.58	60.8	76.3	1.94	1.70	227	30
		Max	518492	572	710	3891	2662	23.0	1.91	60834	11.7	2.96	2.93	2.73	0.417	1.63	236	5.94	51.1	178	4974	22.6	99.0	35279	4001
		n	100	100	100	100	86	80	100	100	80	51	99	48	100	79	100	79	92	100	100	100	100	99	86
24-2551-01	Pyrite All Veins	Min	261275	0.034	0.129	2.97	0.016	0.003	0.099	46.2	0.020	0.004	0.004	0.010	0.001	0.004	0.061	0.003	0.003	0.051	0.072	0.004	0.044	0.331	0.031
		Median	418743	114	285	51.7	2.15	0.277	0.405	27774	3	0.054	0.307	0.254	0.055	0.261	22.7	0.929	2.26	32.7	62.3	4.70	2.15	88.3	27.4
		Max	583522	11708	7693	3891	2662	23.0	9.9	60834	12	6.19	7.67	2.73	0.417	2.11	991	9.9	51.1	248	4974	129	99.0	35279	5688
		n	260	260	260	260	226	221	260	260	231	127	254	146	248	217	260	237	248	260	260	260	260	254	226

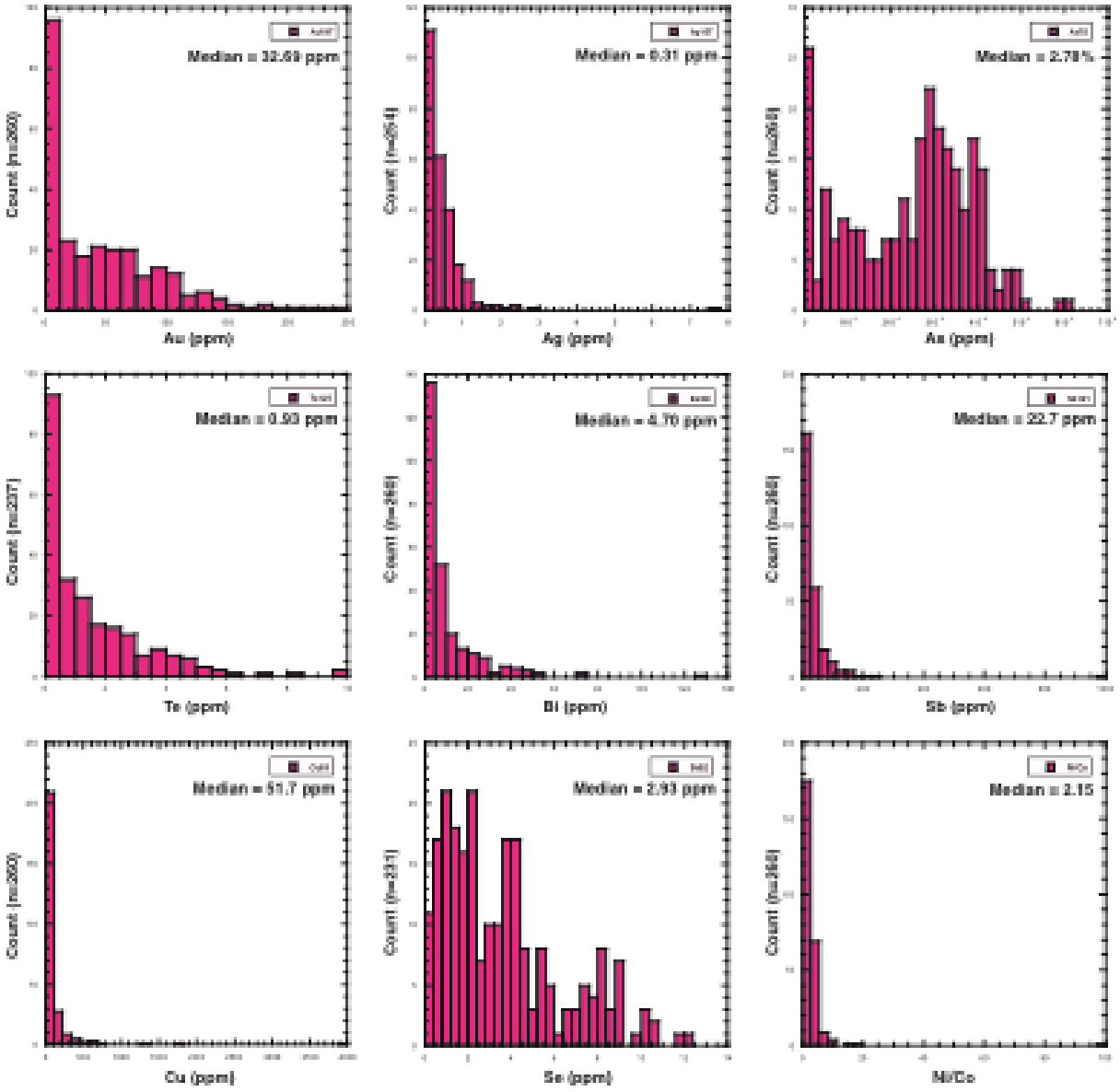

Figure 4: Summary histograms of pyrite trace-element signatures obtained by Laser Ablation ICP-MS analyses, DDH 24-2551-01 (See Table 3).

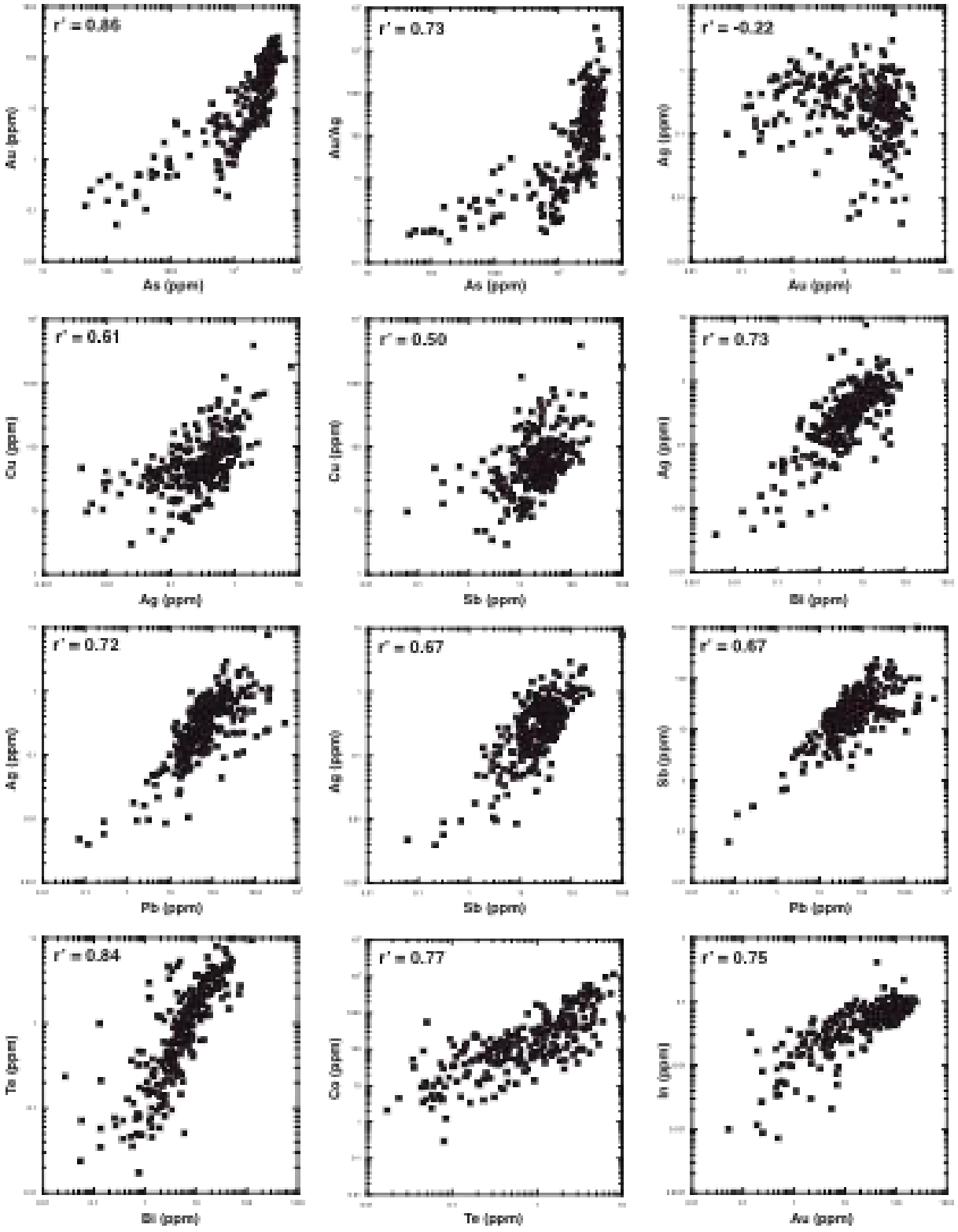

Figure 5: Summary bivariate plots for pyrite trace-element signatures obtained by Laser Ablation ICP-MS analyses, DDH 24-2551-01 (See Table 3). Trends exhibit correlative behaviour between element pairs; Spearman Rank Correlation coefficients (r') quantify the strength of a correlation (99% Confidence, n= 260, r'_{crit}>0.14).

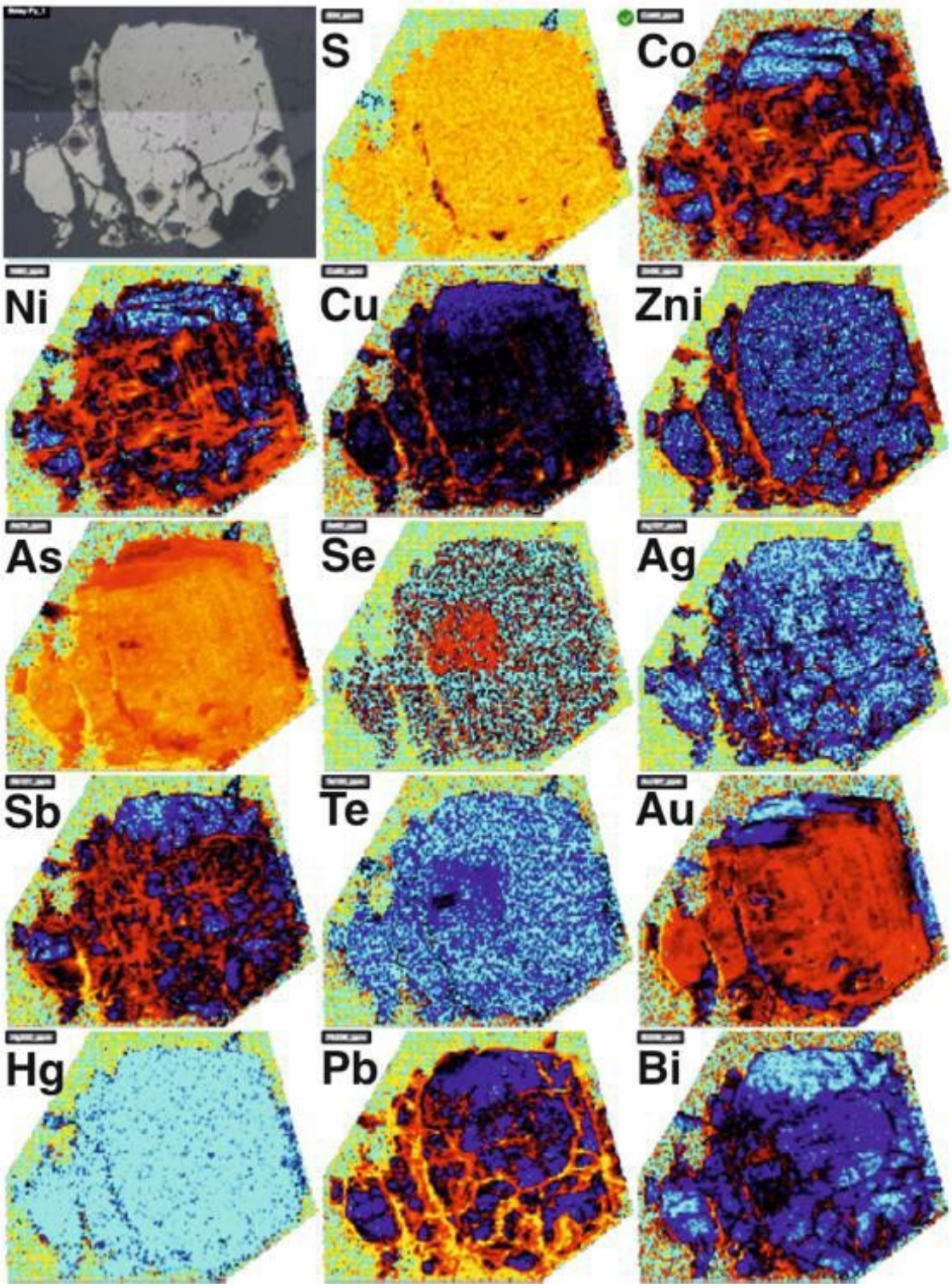

Figure 6: Laser Ablation ICP-MS element maps (colour rendering) of a pyrite grain from DDH 24-2551. Maps exhibit refractory signatures as well as minor remobilization during tectonism. Ablation pits for corresponding spot analyses (See Table 3) are visible in reflected light image (Top Left).

Conclusions:

Lithological reassessment of intervals from DDH 24-2551-01 identified several sulphide bearing quartz veins with potential for the detection of trace hydrothermal signatures for potential Au fertility and vectoring assessment. Petrographic examination of polished sections reveal a broad mineralogical association of Chalcopyrite-Galena-Pyrite-Arsenopyrite prospective for Au mineralization. Microscopic confirmation of quartz-vein hosted lode gold in bedrock intersected by IMC Exploration drillhole 24-2551-01 at a depth of 90.5m. Microscopic examination of Boley sections reveals a high abundance of Bismuth-Tellurides and Tetrahedrite associated with Chalcopyrite and Au grains. Electron Dispersive X-ray analyses reveal an Au-rich Electrum ($Au_{91}Ag_{09}$) composition for the Au grains identified in polished Boley Sections from veins at 90.5m. Mineralogical signature is indicative of an Orogenic Au signature consistent with regional occurrence of visible Au grains in quartz veins across PL2551. Laser-Ablation ICP-MS analyses of pyrite reveal significant enrichment of Au up to 248 g/t (8.7 Oz/ton) representing among the highest recorded Pyrite-Au signatures for Caledonian terranes, with average values of 32.7 g/t Au spanning a broad zone between depths of 88.5 m and 139.7m; signatures are similar to pyrite phases hosting Au at the Curraghinalt deposit, Dalradian Terrane. Mineralogical and micro-analytical assessment of the Boley Quartz veins indicate significant Au fertility in the region and the presence of broader orogenic Au mineralization. Discrete Au-bearing quartz veins intersected in drillhole 24-2551-01 likely represent the distal extent of a larger orogenic gold trend. Abundance of pyrite and chalcopyrite in quartz veins prove to be the most effective vectors for exploration on PL2551. Lithogeochemical vectoring should focus on Bi, Te, Cu, As, Sb, Pb, Ag and Au as vectors toward orogenic Au mineralization.